

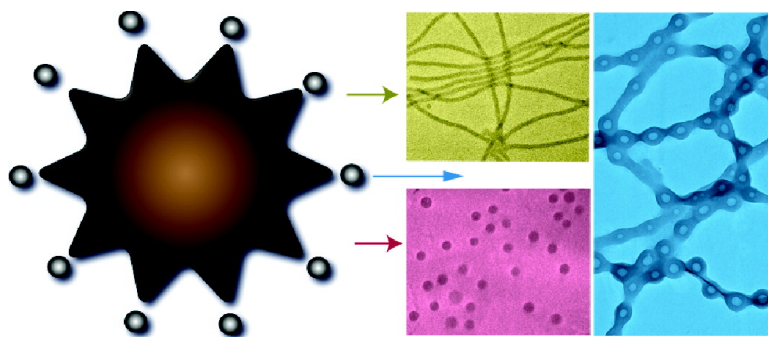
Article

Spontaneous Generation of Amphiphilic Block Copolymer Micelles with Multiple Morphologies through Interfacial Instabilities

Jintao Zhu, and Ryan C. Hayward

J. Am. Chem. Soc., 2008, 130 (23), 7496-7502 • DOI: 10.1021/ja801268e • Publication Date (Web): 15 May 2008

Downloaded from <http://pubs.acs.org> on February 8, 2009



More About This Article

Additional resources and features associated with this article are available within the HTML version:

- Supporting Information
- Links to the 3 articles that cite this article, as of the time of this article download
- Access to high resolution figures
- Links to articles and content related to this article
- Copyright permission to reproduce figures and/or text from this article

[View the Full Text HTML](#)

Spontaneous Generation of Amphiphilic Block Copolymer Micelles with Multiple Morphologies through Interfacial Instabilities

Jintao Zhu and Ryan C. Hayward*

*Polymer Science and Engineering Department, University of Massachusetts,
Amherst, Massachusetts 01003*

Received February 27, 2008; E-mail: rhayward@mail.pse.umass.edu

Abstract: We introduce a method for the formation of block copolymer micelles through interfacial instabilities of emulsion droplets. Amphiphilic polystyrene-block-poly(ethylene oxide) (PS-PEO) copolymers are first dissolved in chloroform; this solution is then emulsified in water and chloroform is extracted by evaporation. As the droplets shrink, the organic solvent/water interface becomes unstable, spontaneously generating a new interface and leading to dispersion of the copolymer as micellar aggregates in the aqueous phase. Depending on the composition of the copolymer, spherical or cylindrical micelles are formed, and the method is shown to be general to polymers with several different hydrophobic blocks: poly(1,4-butadiene), poly(ϵ -caprolactone), and poly(methyl methacrylate). Using this method, hydrophobic species dissolved or suspended in the organic phase along with the amphiphilic copolymer can be incorporated into the resulting micelles. For example, addition of PS homopolymer, or a PS-PEO copolymer of different composition and molecular weight, allows the diameter and morphology of wormlike micelles to be tuned, while addition of hydrophobically coated iron oxide nanoparticles enables the preparation of magnetically loaded spherical and wormlike micelles.

1. Introduction

The self-assembly of amphiphilic molecules into discrete micellar nano-objects is important in areas such as nanoscale materials synthesis,¹ nanolithography,² and drug delivery.^{3–5} Compared to small-molecular-weight surfactants and lipids, block copolymers offer greater flexibility for controlling micellar structure and functionality through choices of polymer composition, architecture, molecular weight, and monomer chemistry.⁶ Polymeric micelles with cylindrical, or wormlike, structures are of particular interest for drug delivery due to their large core capacities and elongated structures, which offer additional opportunities to control biodistribution and release profiles of therapeutic agents.^{4,7–12} Recent work on cylindrical micelles has

established a remarkably fine level of control over morphology, enabling preparation of, e.g., core-shell-corona structures,^{13–15} segmented micelles,^{16–18} and helices.¹⁹

In practice, amphiphilic block copolymer micelles are prepared via one of two general routes. For polymers with sufficiently short and mobile core-forming blocks, the polymer can be directly dissolved from the “melt” (i.e., a bulk sample or dried film) into a solvent which is selective for the corona block.^{16,20–25} For polymers with high molecular weight, glassy, or semicrystalline core blocks, the ability of the polymer to

- (1) Förster, S.; Konrad, M. *J. Mater. Chem.* **2003**, *13* (11), 2671–2688.
- (2) Glass, R.; Möller, M.; Spatz, J. P. *Nanotechnology* **2003**, *14* (10), 1153–1160.
- (3) Rösler, A.; Vandermeulen, G. W. M.; Klok, H. A. *Adv. Drug Delivery Rev.* **2001**, *53* (1), 95–108.
- (4) Dalhaimer, P.; Engler, A. J.; Parthasarathy, R.; Discher, D. E. *Biomacromolecules* **2004**, *5* (5), 1714–1719.
- (5) Gaucher, G.; Dufresne, M. H.; Sant, V. P.; Kang, N.; Maysinger, D.; Leroux, J. C. *J. Controlled Release* **2005**, *109* (1–3), 169–188.
- (6) Riess, G. *Prog. Polym. Sci.* **2003**, *28* (7), 1107–1170.
- (7) Geng, Y.; Discher, D. E. *J. Am. Chem. Soc.* **2005**, *127* (37), 12780–12781.
- (8) Geng, Y.; Discher, D. E. *Polymer* **2006**, *47* (7), 2519–2525.
- (9) Kim, Y.; Dalhaimer, P.; Christian, D. A.; Discher, D. E. *Nanotechnology* **2005**, *16* (7), S484–S491.
- (10) Giacomelli, C.; Schmidt, V.; Borsali, R. *Macromolecules* **2007**, *40* (6), 2148–2157.
- (11) Lodge, T. P.; Rasdal, A.; Li, Z. B.; Hillmyer, M. A. *J. Am. Chem. Soc.* **2005**, *127* (50), 17608–17609.
- (12) Geng, Y.; Dalhaimer, P.; Cai, S. S.; Tsai, R.; Tewari, M.; Minko, T.; Discher, D. E. *Nat. Nanotechnol.* **2007**, *2* (4), 249–255.

- (13) Lei, L. C.; Gohy, J. F.; Willet, N.; Zhang, J. X.; Varshney, S.; Jérôme, R. *Macromolecules* **2004**, *37* (3), 1089–1094.
- (14) Chen, Z. Y.; Cui, H. G.; Hales, K.; Li, Z. B.; Qi, K.; Pochan, D. J.; Wooley, K. L. *J. Am. Chem. Soc.* **2005**, *127* (24), 8592–8593.
- (15) Thünemann, A. F.; Kubowicz, S.; von Berlepsch, H.; Möhwald, H. *Langmuir* **2006**, *22* (6), 2506–2510.
- (16) Li, Z. B.; Kesselman, E.; Talmon, Y.; Hillmyer, M. A.; Lodge, T. P. *Science* **2004**, *306* (5693), 98–101.
- (17) Cui, H. G.; Chen, Z. Y.; Zhong, S.; Wooley, K. L.; Pochan, D. J. *Science* **2007**, *317* (5838), 647–650.
- (18) Wang, X. S.; Guerin, G.; Wang, H.; Wang, Y. S.; Manners, I.; Winnik, M. A. *Science* **2007**, *317* (5838), 644–647.
- (19) Zhong, S.; Cui, H. G.; Chen, Z. Y.; Wooley, K. L.; Pochan, D. J. *Soft Matter* **2008**, *4* (1), 90–93.
- (20) Jain, S.; Bates, F. S. *Science* **2003**, *300* (5618), 460–464.
- (21) Jain, S.; Bates, F. S. *Macromolecules* **2004**, *37* (4), 1511–1523.
- (22) Brannan, A. K.; Bates, F. S. *Macromolecules* **2004**, *37* (24), 8816–8819.
- (23) Nikova, A. T.; Gordon, V. D.; Cristobal, G.; Talingting, M. R.; Bell, D. C.; Evans, C.; Joanicot, M.; Zasadzinski, J. A.; Weitz, D. A. *Macromolecules* **2004**, *37* (6), 2215–2218.
- (24) Zupancich, J. A.; Bates, F. S.; Hillmyer, M. A. *Macromolecules* **2006**, *39* (13), 4286–4288.
- (25) Liu, G. J.; Yan, X. H.; Duncan, S. *Macromolecules* **2002**, *35* (26), 9788–9793.

reorganize is often insufficient to permit direct dissolution in this manner. In these cases, the polymers are typically dissolved in an organic solvent that solvates both blocks; addition of a selective solvent for the corona block (typically water) then drives the polymer to self-assemble into micellar aggregates.^{6,26–32} This approach relies on a controlled “precipitation” of the core block due to addition of the nonsolvent, and careful control of mixing conditions allows other hydrophobic ingredients to be coprecipitated with the amphiphilic polymers, resulting in micelles that encapsulate therapeutic molecules^{33,34} and nanoparticles^{35–37} for imaging³⁸ or magnetic targeting.³⁹ Notably, while nanoparticles have been successfully incorporated into hydrophilic portions of cylindrical micelles,^{17,40} we are not aware of any reports of encapsulation of hydrophobic nanoparticles within wormlike micelle cores. Apparently, the same conditions of rapid precipitation that promote incorporation of nanoparticles into micelles do not easily allow for the growth of extended cylindrical micellar structures.

Here, we introduce a new route to the formation of polymeric micelles that takes advantage of interfacial instabilities in shrinking emulsion droplets containing amphiphilic diblock copolymers. Instead of dissolving the copolymer in a water-miscible solvent, we use a water-immiscible organic solvent (chloroform) which is a good solvent for both blocks of the copolymer. This polymer solution is next dispersed as emulsion droplets in a continuous aqueous phase, followed by removal of solvent from the droplets by diffusion through the aqueous phase and evaporation. As the content of copolymer within the droplets increases, self-assembly of the polymer takes place through a series of interfacial instabilities, wherein the droplets spontaneously increase in surface area and ultimately eject micellar assemblies into the aqueous phase. We note that a similar procedure—dispersion of chloroform-containing amphiphilic polymer in water—has been previously employed by Discher and co-workers to prepare wormlike micelles of poly(ϵ -caprolactone)-*b*-PEO (PCL-PEO),^{7,8} however the mechanism of micelle formation in this system has not been reported. Here, we show that the generation of polymeric micelles through

Table 1. Characteristics of the Micelle-Forming Copolymers Employed in This Study^a

copolymer	M_n (kg/mol)	M_w/M_n	w_{EO}	structure
PS _{9.5k} -PEO _{18.0k}	27.5	1.09	0.65	S
PS _{9.5k} -PEO _{9.5k}	19.0	1.07	0.50	S/W
PS _{9.5k} -PEO _{5.0k}	14.5	1.05	0.34	W
PCL _{10.0k} -PEO _{5.0k}	15.0	1.33	0.33	W/V
PB _{11.8k} -PEO _{5.3k}	17.1	1.04	0.31	W/V
PMMA _{11.0k} -PEO _{11.0k}	22.0	1.24	0.50	W

^a S: spherical micelles. W: wormlike micelles. V: vesicles/lamellar structures.

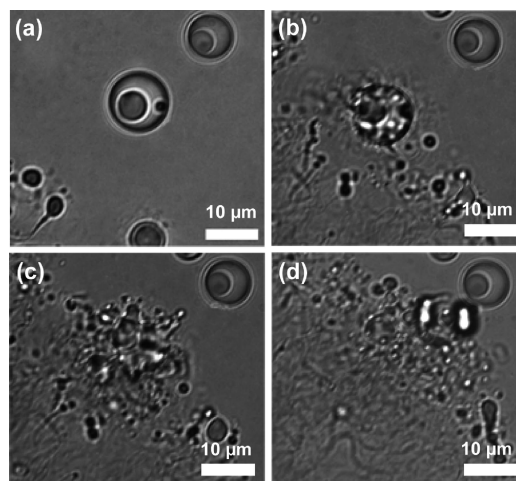


Figure 1. Formation of wormlike micelles proceeds via an interfacial instability of shrinking chloroform-in-water emulsion droplets containing PS_{9.5k}-PEO_{5.0k}. The time elapsed between the optical micrograph in (a) and subsequent images was (b) 24 s, (c) 26 s, and (d) 30 s.

interfacial instabilities is applicable to polymers with a wide range of compositions and allows multiple components to be easily incorporated within compound micellar structures. In particular, this approach allows us to fabricate giant wormlike micelles of glassy polymers that have easily tunable diameters, novel internal structures, and encapsulated iron oxide nanoparticles.

2. Results and Discussion

2.1. Interfacial Instabilities. Interfacial instabilities in shrinking emulsion droplets were investigated using three amphiphilic polystyrene-block-poly(ethylene oxide) (PS-PEO) copolymers with a constant PS molecular weight (9.5 kg/mol) and varying PEO molecular weight, as summarized in Table 1. The copolymers were first dissolved in chloroform—a good solvent for both PS and PEO and only slightly miscible with water—followed by emulsification of polymer solutions in water containing poly(vinyl alcohol) (PVA) as a surfactant to stabilize the droplets (for experimental details see the Supporting Information). The droplets often consist of water-in-chloroform-in-water double emulsions, as seen in Figure 1a, since the PS-PEO polymers themselves can act to stabilize water-in-oil emulsions.⁴¹ After allowing the droplets to sediment, emulsions were left in an open container so that chloroform could diffuse through the aqueous phase and evaporate at the air-water

(41) The emulsion initially consists almost entirely of chloroform-in-water droplets, with the double emulsion structure emerging only as the droplets shrink and become supersaturated with water. Presumably this behavior reflects the increasing surface activity of PS-PEO copolymers as their concentration within the droplets increases.

- (26) Zhang, L. F.; Eisenberg, A. *J. Am. Chem. Soc.* **1996**, *118* (13), 3168–3181.
- (27) Zhang, L. F.; Eisenberg, A. *J. Polym. Sci., Part B: Polym. Phys.* **1999**, *37* (13), 1469–1484.
- (28) Shen, H. W.; Zhang, L. F.; Eisenberg, A. *J. Am. Chem. Soc.* **1999**, *121* (12), 2728–2740.
- (29) Erhardt, R.; Zhang, M. F.; Böker, A.; Zettl, H.; Abetz, C.; Frederik, P.; Krausch, G.; Abetz, V.; Müller, A. H. E. *J. Am. Chem. Soc.* **2003**, *125* (11), 3260–3267.
- (30) Liu, G. J. *Adv. Mater.* **1997**, *9* (5), 437–439.
- (31) Kubowicz, S.; Baussard, J. F.; Lutz, J. F.; Thünemann, A. F.; von Berlepsch, H.; Laschewsky, A. *Angew. Chem., Int. Ed.* **2005**, *44* (33), 5262–5265.
- (32) Gohy, J. F.; Willet, N.; Varshney, S.; Zhang, J. X.; Jérôme, R. *Angew. Chem., Int. Ed.* **2001**, *40* (17), 3214–3216.
- (33) Park, E. K.; Lee, S. B.; Lee, Y. M. *Biomaterials* **2005**, *26* (9), 1053–1061.
- (34) Giacomelli, C.; Schmidt, V.; Borsali, R. *Langmuir* **2007**, *23* (13), 6947–6955.
- (35) Kim, B. S.; Qiu, J. M.; Wang, J. P.; Taton, T. A. *Nano Lett.* **2005**, *5* (10), 1987–1991.
- (36) Sanchez-Gaytan, B. L.; Cui, W. H.; Kim, Y. J.; Mendez-Polanco, M. A.; Duncan, T. V.; Fryd, M.; Wayland, B. B.; Park, S. J. *Angew. Chem., Int. Ed.* **2007**, *46* (48), 9235–9238.
- (37) Yusuf, H.; Kim, W. G.; Lee, D. H.; Guo, Y. Y.; Moffitt, M. G. *Langmuir* **2007**, *23* (2), 868–878.
- (38) Ai, H.; Flask, C.; Weinberg, B.; Shuai, X.; Pagel, M. D.; Farrell, D.; Duerk, J.; Gao, J. M. *Adv. Mater.* **2005**, *17* (16), 1949–1952.
- (39) Safarik, I.; Safarikova, M. *Monatsh. Chem.* **2002**, *133* (6), 737–759.
- (40) Wang, H.; Lin, W. J.; Fritz, K. P.; Scholes, G. D.; Winnik, M. A.; Manners, I. *J. Am. Chem. Soc.* **2007**, *129* (43), 12924–12925.

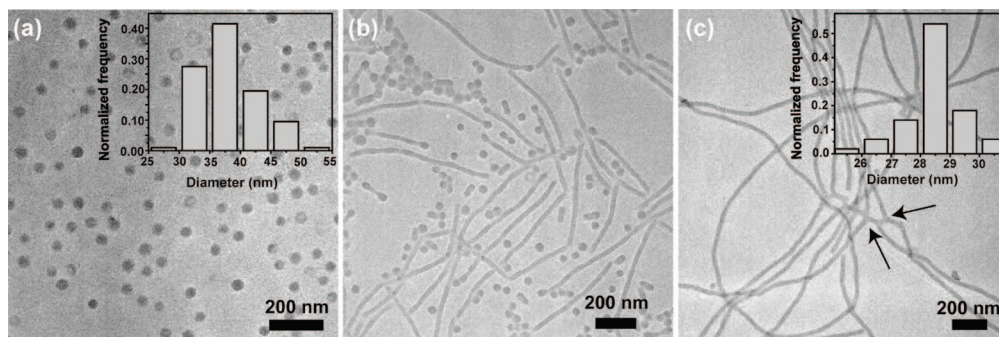


Figure 2. Bright field TEM images of micelles formed through interfacial instabilities of emulsion droplets containing amphiphilic block copolymers: (a) spherical micelles of PS_{9.5k}-PEO_{18.0k}, $w_{EO} = 0.65$; (b) mixed spherical/wormlike micelles of PS_{9.5k}-PEO_{9.5k}, $w_{EO} = 0.50$; (c) extended wormlike micelles of PS_{9.5k}-PEO_{5.0k}, $w_{EO} = 0.34$, with arrows denoting branching points. Insets in (a) and (c) show the distributions of measured micelle diameters.

interface. As the droplets shrank, the concentration of PS-PEO increased, eventually triggering an instability of the organic/water interface. As shown in Figure 1 for PS_{9.5k}-PEO_{5.0k}, when the concentration of copolymer in the droplets reached ~ 40 wt %, the droplet surfaces became rough and, over a period of seconds, spontaneously divided into smaller ($< 1 \mu\text{m}$) droplets and threads, as shown in Figure 1b-d (and Supporting Information, Movie 1). Ultimately, PS_{9.5k}-PEO_{5.0k} was almost completely dispersed in the aqueous phase as wormlike micelles, as we describe below. Similar instabilities were observed for the other polymers listed in Table 1 (see also Supporting Information, Movie 2), though the details of the process and the micellar morphology depend sensitively on the composition of the copolymer.

The observed instabilities are apparently examples of “spontaneous emulsification”^{42,43} wherein the presence of highly surface-active species leads to roughening of the interface between immiscible fluids and formation of small droplets.^{42,44–49} Such instabilities may occur whenever a ternary liquid/liquid/amphiphile system whose equilibrium state is a microemulsion is initially prepared in a macroscopically phase-separated state. The strong driving force for adsorption of the amphiphilic molecules to the interface between the immiscible liquids gives rise to a vanishing or transiently negative interfacial tension between the two bulk phases, thereby triggering spontaneous creation of interface and allowing the system to evolve toward its equilibrium microemulsion structure.⁴⁴ In the current system, the macrophase-separated state, with water as one phase and chloroform containing a dilute concentration of PS-PEO as the other, is initially stable (or more precisely, metastable, since the chloroform phase is dispersed as emulsion droplets). However, as solvent is removed from the droplets, the system presumably becomes “quenched” into a composition regime where the equilibrium structure is a microemulsion consisting of chloroform-swelled PS-PEO assemblies dispersed in water.

This triggers the onset of an interfacial instability, the subsequent evolution of which depends on the properties of the amphiphilic copolymer, in particular the polymer’s preferred interfacial curvature.

2.2. Structures of PS-PEO Micelles. The micellar structures of PS-PEO copolymers generated through interfacial instabilities were studied via transmission electron microscopy (TEM), as shown in Figure 2. Using PS_{9.5k}-PEO_{18.0k} (weight fraction of PEO, $w_{EO} = 0.65$) spherical micelles with diameters of 38 ± 4.5 nm were generated (Figure 2a). As these measurements were performed on dried samples, the values include the size of the collapsed PEO coronae, and the stated uncertainty reflects the standard deviation of a normal distribution fitted to the histogram of micelle sizes (Figure 2a, inset). A decrease in molecular weight of the PEO block to PS_{9.5k}-PEO_{9.5k} ($w_{EO} = 0.50$) gave rise to a mixture of spherical and cylindrical micelles, as shown in Figure 2b. The spherical micelles had diameters of 39 ± 5 nm while the coexisting wormlike micelles had diameters of 28 ± 3 nm. The wormlike micelles were typically short, with contour lengths from ~ 100 nm to $\sim 3 \mu\text{m}$. A further decrease in the length of the hydrophilic PEO block to PS_{9.5k}-PEO_{5.0k} ($w_{EO} = 0.34$) yielded almost exclusively wormlike micelles with diameters of 29 ± 1 nm (Figure 2c) and contour lengths of up to several tens of microns. Occasionally, branches in the micelles were observed, as indicated by the arrows in Figure 2c. Despite the fact that these structures are clearly not at equilibrium (due to the glassy nature of PS at room temperature), the observed morphologies agree well with the previously reported equilibrium phase diagram for polybutadiene-PEO copolymers.²⁰ We note that for smaller weight fractions of PEO in the copolymers ($w_{EO} \sim 0.25$), where one would expect vesicular structures in the equilibrium phase diagram,²⁰ the observed interfacial instabilities gave rise to hierarchically structured microparticles with PS-PEO copolymers locally arranged into bilayers.⁵⁰

2.3. Generality of the Method. To test the generality of the approach of generating micellar structures through interfacial instabilities, we studied the behavior of three amphiphilic block copolymers with different hydrophobic blocks: poly(ϵ -caprolactone)-*b*-PEO (PCL_{10.0k}-PEO_{5.0k}), poly(1,4-butadiene)-*b*-PEO, (PB_{11.8k}-PEO_{5.3k}), and poly(methyl methacrylate)-*b*-PEO (PMMA_{11.0k}-PEO_{11.0k}), as summarized in Table 1. Indeed, upon extraction of chloroform from emulsion droplets containing each of these copolymers, we observed interfacial instabilities similar to those described above. The end result for PCL_{10.0k}-PEO_{5.0k} ($w_{EO} = 0.33$) was a mixture of giant wormlike micelles with

(42) López-Montilla, J. C.; Herrera-Morales, P. E.; Pandey, S.; Shah, D. O. *J. Dispersion Sci. Technol.* **2002**, *23* (1–3), 219–268.

(43) López-Montilla, J. C.; Herrera-Morales, P. E.; Shah, D. O. *Langmuir* **2002**, *18* (11), 4258–4262.

(44) Granek, R.; Ball, R. C.; Cates, M. E. *J Phys II* **1993**, *3* (6), 829–849.

(45) Granek, R. *Langmuir* **1996**, *12* (21), 5022–5027.

(46) Jiao, J. B.; Kramer, E. J.; de Vos, S.; Möller, M.; Koning, C. *Macromolecules* **1999**, *32* (19), 6261–6269.

(47) Jiao, J. B.; Kramer, E. J.; de Vos, S.; Möller, M.; Koning, C. *Polymer* **1999**, *40* (12), 3585–3588.

(48) Kim, B. J.; Kang, H. M.; Char, K.; Katsov, K.; Fredrickson, G. H.; Kramer, E. J. *Macromolecules* **2005**, *38* (14), 6106–6114.

(49) Girard-Reydet, E.; Pascault, J. P.; Brown, H. R. *Macromolecules* **2001**, *34* (15), 5349–5353.

(50) Zhu, J. T.; Hayward, R. C. *Angew. Chem., Int. Ed.* **2008**, *47* (11), 2113–2116.

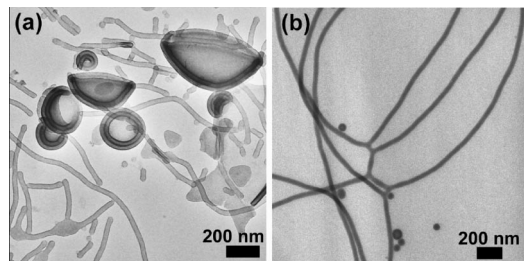


Figure 3. Micellar assemblies of amphiphilic copolymers with a variety of hydrophobic blocks were formed through interfacial instabilities. Bright field TEM images revealed (a) wormlike micelles along with vesicular and lamellar structures of PCL_{10.0k}-PEO_{5.0k} ($w_{EO} = 0.33$), negatively stained by 1 wt % aqueous PTA solution, and (b) wormlike micelles of PB_{11.8k}-PEO_{5.3k} ($w_{EO} = 0.31$), fixed and stained by addition of 0.05 wt % OsO₄ to the micelle solution.

vesicles and lamellar structures, while PB_{11.8k}-PEO_{5.3k} ($w_{EO} = 0.31$) formed mostly wormlike micelles with some small vesicles, as seen in Figure 3. For PMMA_{11.0k}-PEO_{11.0k} ($w_{EO} = 0.50$), predominantly wormlike micelles were formed, though they were more variable in diameter and more highly branched than with the other copolymers (Supporting Information, Figure SI-1). We note that the choice of organic solvent is quite important; for example, the use of toluene or benzene tends to suppress interfacial instabilities, ultimately leading to formation of micrometer-sized particles with internal structures. We hypothesize that the key parameter is the quality of the organic solvent for the hydrophilic block. Toluene or benzene (good solvents for PEO, though of lower quality than chloroform) may promote aggregation of the copolymer, thereby limiting its ability to adsorb to the interface and preventing the interfacial tension from falling to zero. However, the sensitivity to solvent type, as well as the behavior of polymers with hydrophilic blocks other than PEO, requires further investigation.

2.4. Controlling Structures of Wormlike Micelles by Blending. A key advantage to using an organic solvent to prepare amphiphilic copolymer micelles is the possibility to incorporate other hydrophobic ingredients, thermodynamically immiscible with the polymer in the bulk, into the micellar cores. When micellization is induced by addition of water to water-miscible organic solvents, care must be taken with regards to the relative solubilities of each component to ensure that the active ingredient does not macroscopically precipitate before micellization takes place, or vice versa.^{36,38} For example, Gindy et al. have shown that, by rapidly mixing the organic phase with water, supersaturation of all hydrophobic components can be achieved, ensuring synchronous precipitation and quantitative incorporation of nanoparticles and hydrophobic molecules into spherical aggregates of PCL-PEO.⁵¹ However, for the case of wormlike micelles, while successful loading with hydrophobic drug molecules has been demonstrated,⁴ a general strategy for encapsulation of other materials, in particular nanoparticles, has not been reported. Presumably, this reflects the difficulty inherent in tuning solvent conditions to simultaneously achieve high-efficiency encapsulation and growth of extended cylindrical structures.

The basic mechanism of micelle formation via interfacial instabilities reported here is completely distinct from the methods relying on controlled precipitation and, as we show below, opens opportunities for formation of wormlike micelles

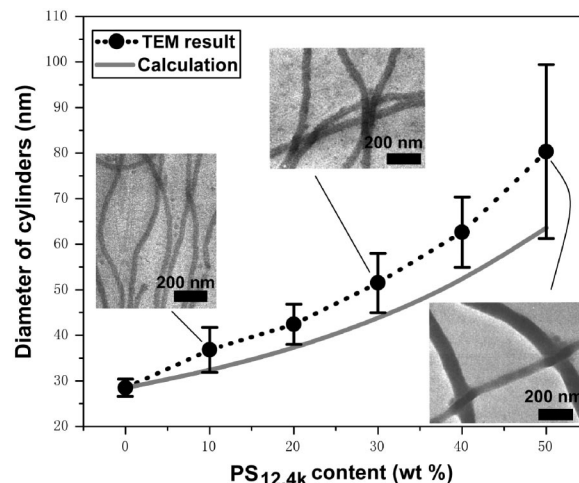


Figure 4. The diameter of wormlike micelles was tuned by adding PS_{12.4k} homopolymer to the solutions of PS_{9.5k}-PEO_{5.0k} in chloroform prior to emulsification. The composition axis represents the weight percentage of polymer in the initial solution constituted by PS_{12.4k}. Markers represent sizes obtained from TEM measurements, while the solid line shows the predicted value based on a constant interfacial area per PS_{9.5k}-PEO_{5.0k} chain (eq 3). Error bars represent the standard deviation of measured micelle diameters. Representative TEM images are shown for selected points (all images are at the same magnification).

with new structures and containing hydrophobic nanoparticles. However, the design principles governing the successful incorporation of components into micelles formed through interfacial instabilities remain to be established. As first steps in this direction, we explore below blends of micelle-forming PS-PEO copolymers with three materials: (i) PS_{12.4k} homopolymer, (ii) PS_{38.0k}-PEO_{11.0k} diblock copolymer, and (iii) iron oxide nanoparticles coated with hydrophobic ligands.

2.4.1. Swelling of Wormlike Micelles by PS Homopolymer.

It has previously been shown that incorporation of homopolymer into the cores of amphiphilic copolymer micelles provides an effective way to tune micellar size^{26,52} and even induce changes in aggregate morphology.^{27,53} Indeed, we found here that the diameter of wormlike micelles can be controlled by dissolving PS_{12.4k} homopolymer in chloroform along with PS_{9.5k}-PEO_{5.0k} prior to emulsification. We studied this effect by keeping the overall polymer concentration fixed at 10 mg/mL and varying the fraction of homopolymer relative to block copolymer. The diameter of the wormlike micelles became larger with increasing PS_{12.4k} content, as shown in Figure 4, while the typical length of micelles remained on the order 10 μ m. The size dispersity of the micelles increased somewhat when homopolymer was added, reflecting variability in the distribution of PS_{12.4k} between different micelles. However, the standard deviations of micelle diameters (indicated by the error bars in Figure 4) remained reasonably small, with a size of 63 ± 8 nm obtained at 40 wt % PS_{12.4k}. At 50 wt % homopolymer, micelles became markedly more polydisperse, with diameters of 80 ± 19 nm. Further increases in the content of PS homopolymer gave rise to wormlike micelles with undulations at 60 wt % (Figure 5a), "pearl necklace" microstructures at 70 wt % (Figure 5b) and polydisperse spherical aggregates (diameters of ~ 60 nm to ~ 1 μ m) at 80 wt % (Figure 5c).

(51) Gindy, M. E.; Panagiotopoulos, A. Z.; Prud'homme, R. K. *Langmuir* **2008**, *24* (1), 83–90.

(52) Whitmore, M. D.; Smith, T. W. *Macromolecules* **1994**, *27* (17), 4673–4683.

(53) Lei, L. C.; Gohy, J. F.; Willet, N.; Zhang, J. X.; Varshney, S.; Jérôme, R. *Polymer* **2004**, *45* (13), 4375–4381.

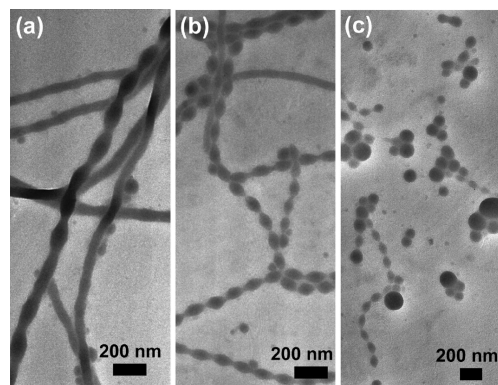


Figure 5. Bright field TEM images of aggregate morphologies formed by blending $\text{PS}_{9.5\text{k}}\text{-PEO}_{5.0\text{k}}$ and $\text{PS}_{12.4\text{k}}$ with weight ratios of (a) 40:60; (b) 30:70; and (c) 20:80, showing the undulation of wormlike micelles and eventual change in structure to polydisperse spherical aggregates at high extents of PS homopolymer loading.

To better understand how the addition of PS homopolymer controls the dimensions of cylindrical micelles, we consider the following simple model. Based on a purely geometric consideration of the surface area to volume ratio of a long cylinder, the interfacial area occupied by each block copolymer chain in the micelles of pure $\text{PS}_{9.5\text{k}}\text{-PEO}_{5.0\text{k}}$ (Σ_{chain}) can be written as

$$\Sigma_{\text{chain}} = \frac{4V_{\text{PS}}}{d_{\text{core}}^0} \quad (1)$$

where V_{PS} represents the volume occupied by the polystyrene block of a single copolymer chain. The diameter of the micelle core, d_{core}^0 , is determined from TEM measurements of (dried) $\text{PS}_{9.5\text{k}}\text{-PEO}_{5.0\text{k}}$ micelles, subtracting the contribution of the PEO corona by assuming that the PS and PEO blocks have densities of 1.05 and 1.15 g/cm^3 , respectively. Upon blending of $\text{PS}_{12.4\text{k}}$ into the micelle cores, the diameter of the composite micelle swells to a new diameter d_{core} , and the same geometric argument gives the interfacial area per copolymer chain as

$$\Sigma_{\text{chain}} = \frac{4V_{\text{PS}}}{\phi d_{\text{core}}} \quad (2)$$

where ϕ is the volume fraction of the micelle core made up by the PS block of the copolymer. To estimate the size of the cylindrical micelles containing blended PS homopolymer, we assume that the interfacial area per copolymer chain is not altered by the addition of homopolymer (i.e., Σ_{chain} is constant), such that

$$d_{\text{core}} = \frac{4V_{\text{PS}}}{\phi \Sigma_{\text{chain}}} = \frac{d_{\text{core}}^0}{\phi} \quad (3)$$

While this simple prediction (the solid line in Figure 4) lies reasonably close to the measured values, it consistently underestimates the sizes of the blend micelles, suggesting that Σ_{chain} must decrease slightly upon addition of PS homopolymer.

Fluorescence images of wormlike micelles with three different diameters containing a hydrophobic fluorescent probe are shown in Figure 6. While the micelles have long contour lengths (ca. 5 to 50 μm) in all cases, the pure $\text{PS}_{9.5\text{k}}\text{-PEO}_{5.0\text{k}}$ micelles (Figure 6a) are highly curved, suggesting a persistence length of several micrometers, while the blends containing 40% $\text{PS}_{12.4\text{k}}$ (Figure 6c) are very straight. However, observation of Brownian motion revealed that even the neat $\text{PS}_{9.5\text{k}}\text{-PEO}_{5.0\text{k}}$ micelles are not flexible but instead move as rigid rods with fixed bends in

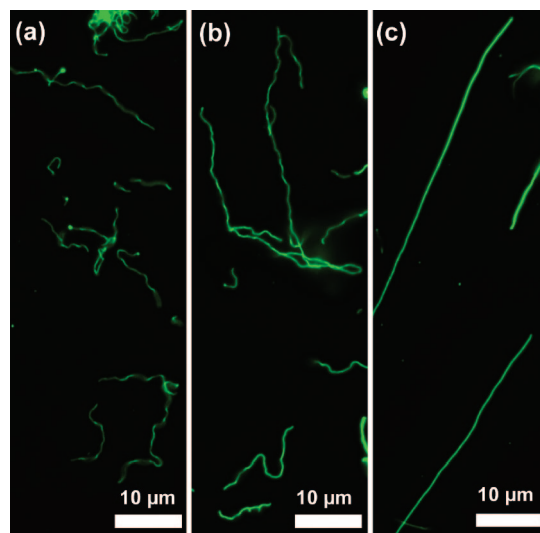


Figure 6. Epi-fluorescence images of cylindrical micelles. (a) For neat $\text{PS}_{9.5\text{k}}\text{-PEO}_{5.0\text{k}}$, the micelle contours exhibit kinetically trapped bends, while thicker micelles formed from blends of $\text{PS}_{9.5\text{k}}\text{-PEO}_{5.0\text{k}}$ and $\text{PS}_{12.4\text{k}}$ with ratios of (b) 80:20 and (c) 60:40 show increasingly straight contours.

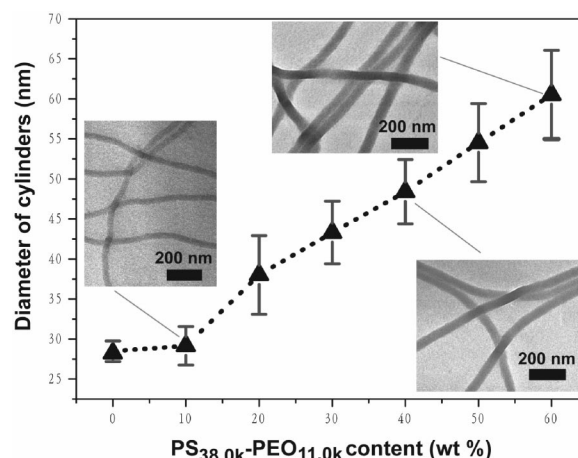


Figure 7. The diameter of wormlike micelles could also be tuned by adding $\text{PS}_{38.0\text{k}}\text{-PEO}_{11.0\text{k}}$ to the solutions of $\text{PS}_{9.5\text{k}}\text{-PEO}_{5.0\text{k}}$ in chloroform prior to emulsification. The composition axis represents the weight percentage of polymer in the initial solution constituted by $\text{PS}_{38.0\text{k}}\text{-PEO}_{11.0\text{k}}$. Error bars represent the standard deviations of measured micelle diameters, indicating that the size distributions remain fairly narrow, even at high contents of $\text{PS}_{38.0\text{k}}\text{-PEO}_{11.0\text{k}}$. Representative TEM images are shown for selected points (all images are at the same magnification).

their contours. Indeed, a simple calculation of the persistence length based on the rigidity of the PS core, $l_p \approx \pi E d_{\text{core}}^4 / 64 k_B T$, where E is Young's modulus (~ 3 GPa for PS) and $k_B T$ is the thermal energy scale, yields $l_p \approx 1$ μm , 3 orders of magnitude larger than the characteristic length scale of bends in the contours of neat $\text{PS}_{9.5\text{k}}\text{-PEO}_{5.0\text{k}}$ micelles, which must therefore reflect the flexibility present in the solvated state before the PS core becomes glassy.

2.4.2. Binary Blends of PS-PEO Block Copolymers. Using the approach presented here, two or more amphiphilic copolymers can be dissolved in the chloroform phase, and under appropriate conditions these copolymers will coassemble through interfacial instabilities into hybrid micelles. In particular, we consider the evolution of $\text{PS}_{9.5\text{k}}\text{-PEO}_{5.0\text{k}}$ wormlike micelle structures upon blending with $\text{PS}_{38.0\text{k}}\text{-PEO}_{11.0\text{k}}$, a chemically analogous copolymer with a larger molecular weight and smaller

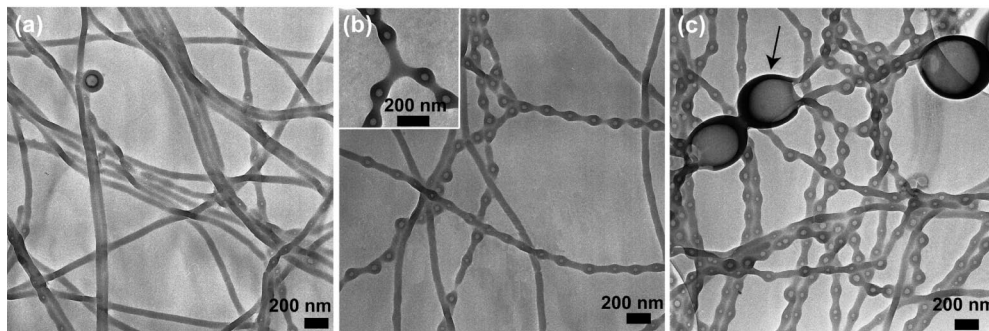


Figure 8. Bright field TEM images showing the evolution of wormlike micellar structure for blends of PS_{9.5k}-PEO_{5.0k} and PS_{38.0k}-PEO_{11.0k} with weight ratios of (a) 30:70; (b) 20:80; and (c) 10:90. Micelles develop internal aqueous compartments which become more closely spaced with greater PS_{38.0k}-PEO_{11.0k} content, yielding strings of small vesicles. In some cases, larger unclosed vesicles were also found along the strings, as indicated by the arrow in (c).

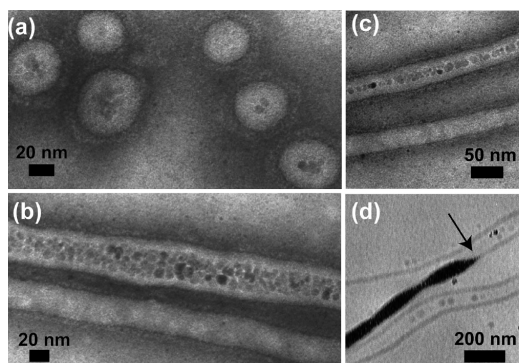


Figure 9. Bright field TEM images of PS-PEO micelles with iron oxide nanoparticles encapsulated in the PS cores: (a) spherical micelles of PS_{9.5k}-PEO_{18.0k}; (b-d) wormlike micelles of PS_{9.5k}-PEO_{9.5k}. In both cases, a fraction of empty micelles not containing iron oxide nanoparticles was observed. Samples (a-c) were negatively stained by 1 wt % PTA aqueous solution.

PEO content ($w_{\text{EO}} = 0.22$). When incorporated into shrinking solvent droplets on its own, PS_{38.0k}-PEO_{11.0k} assembles into complex microparticle structures where the copolymer is locally organized into bilayers, in keeping with the lower content of the hydrophilic PEO block.⁵⁰ Here, we found that droplets containing mixtures of PS_{38.0k}-PEO_{11.0k} with PS_{9.5k}-PEO_{5.0k} still gave rise to instabilities that generated long (tens of micrometers) wormlike micelles with diameters that grew with increasing PS_{38.0k}-PEO_{11.0k} content, as indicated in Figure 7. Remarkably, even at 60 wt % PS_{38.0k}-PEO_{11.0k}, the micelles remained fairly uniform in size (diameter 61 ± 6 nm), suggesting that the two copolymers remain well-mixed throughout the compound aggregates.

Further increases in the PS_{38.0k}-PEO_{11.0k} content of the blends to 70–90 wt % led to a change in micellar morphology, wherein the wormlike micelles developed internal hydrated PEO compartments and undulating shapes—essentially forming a string of small vesicles—as seen in Figure 8. At 70 wt %, these compartments were widely and irregularly spaced, but they became more frequent with increasing PS_{38.0k}-PEO_{11.0k} content, until, at 90 wt % (Figure 7c), they showed a fairly regular spacing of ca. 90 nm. Occasionally, larger, unclosed vesicles (diameter ~ 300 nm) were found along the strings, as indicated by arrows in Figure 8c. Presumably, these “string of vesicle” morphologies reflect a localized phase separation of the two copolymers within the compound micellar structure, as dictated by the different preferred interfacial curvature of the two copolymers. An understanding of whether this structure is close

to equilibrium, or simply represents a kinetically trapped intermediate state, will require detailed theoretical treatment.

2.4.3. Encapsulation of Magnetic Nanoparticles. Magnetic nanoparticles have received considerable attention for biomedical applications, as contrast enhancement agents for magnetic resonance imaging³⁸ and for targeted drug delivery through the use of magnetic fields.³⁹ Several groups have reported the encapsulation of nanoparticles into block copolymer micelles,^{35,38,54,55} where the hydrophobic core of the micelle serves as a carrier for the active ingredients and nanoparticles, while the hydrophilic shell acts as a protective corona. To study the encapsulation of nanoparticles within micelles formed by interfacial instabilities, we added 1–10 wt % (relative to PS-PEO) of ~ 10 nm diameter iron oxide nanoparticles coated with fatty acid ligands to the initial solutions of copolymer in chloroform. Using PS_{9.5k}-PEO_{18.0k}, iron oxide nanoparticles were successfully encapsulated into spherical micelles, as demonstrated by the TEM image in Figure 9a. With PS_{9.5k}-PEO_{9.5k}, the addition of nanoparticles caused a shift in the observed morphology from a mixture of spherical and cylindrical micelles (Figure 2b) to primarily extended wormlike micelles containing iron oxide particles, as shown in Figure 9b–d. The samples shown in Figure 9a–c were negatively stained using a phosphotungstic acid (PTA) aqueous solution, leaving the PS cores bright while staining the PEO coronae dark, and clearly revealing that the nanoparticles segregate to the center of the micelles and are coated with a PS shell. For both copolymers, distributions of the number of particles per micelle were fairly broad, with a fraction of the micelles not containing any nanoparticles. For wormlike micelles of PS_{9.5k}-PEO_{9.5k}, the most commonly observed morphology was cylindrical clusters several nanoparticles in diameter within the PS core (Figure 9b). However, in some cases, a single-file line of particles in the center of the micelle was observed (Figure 9c), while, in other cases, the distribution of particles along a single micelle was discontinuous, including abrupt transitions from “empty” to densely packed with nanoparticles (Figure 9d, arrow). By separating out large aggregates of nanoparticles using a permanent magnet, we estimated that approximately half of the iron oxide particles present in the initial solution were successfully encapsulated within micelles. While a more thorough understanding of the process of micelle formation through interfacial instabilities is needed to improve the

(54) Kang, Y. J.; Taton, T. A. *Angew. Chem., Int. Ed.* **2005**, *44* (3), 409–412.

(55) Euliss, L. E.; Grancharov, S. G.; O'Brien, S.; Deming, T. J.; Stucky, G. D.; Murray, C. B.; Held, G. A. *Nano Lett.* **2003**, *3* (11), 1489–1493.

homogeneity of nanoparticle distribution, we emphasize that it provides a simple and flexible route to encapsulate nanoparticles within wormlike micelles.

3. Conclusion

In summary, we have studied the spontaneous formation of PS-PEO block copolymer micelles via interfacial instabilities of shrinking solvent droplets. This method, which represents a fundamentally different mechanism for micelle formation than those employed previously, allows for preparation of either spherical or wormlike micelles and can be applied to a range of copolymers with different hydrophobic blocks. The diameter of wormlike micelles can be tuned simply by blending with PS homopolymer or another PS-PEO copolymer, which are distributed quite uniformly throughout the micelles up to loadings of 40 and 60 wt %, respectively. In the latter case, further addition of the second PS-PEO copolymer gave rise to wormlike micelle structures with internal aqueous compartments. In a similar fashion, iron oxide nanoparticles with hydrophobic ligands were

successfully incorporated into the PS domains of both spherical and wormlike micelles, simply by adding nanoparticles to the starting polymer solution. While the underlying mechanism and the limitations of this technique require further study, it apparently represents a quite versatile means to prepare micelles from a range of different amphiphilic block copolymers and that contain a variety of encapsulated polymers, active ingredients, and nanoparticles.

Acknowledgment. We gratefully acknowledge funding for this work provided by the National Science Foundation through Grant CBET 0741885 and the MRSEC at UMass (DMR 0213695), as well as the Center for UMass-Industry Research on Polymers.

Supporting Information Available: Experimental details, additional TEM images, and movies showing the spontaneous formation of micelles from emulsion droplets containing PS-PEO. This material is available free of charge via the Internet at <http://pubs.acs.org>.

JA801268E